Wind adaptive urban seafront buildings design for improving urban ventilation and pedestrian wind comfort in Mediterranean climate

Hakan Bas*

The Graduate School of Natural and Applied Sciences,
Dokuz Eylul University,
Tinaztepe Kampusu, 35160, Izmir, Turkey
Email: hakan.bas@ikc.edu.tr
*Corresponding author

Ilknur Turkseven Dogrusoy

Department of Architecture,
Dokuz Eylul University,
Tinaztepe Kampusu, 35160, Izmir, Turkey
Email: ilknur.turkseven@deu.edu.tr

Sigrid Reiter

Local Environment Management and Analysis (LEMA),
University of Liege,
Allée de la Découverte 9 (Bât. B52), 4000, Liege, Belgium
Email: sigrid.reiter@uliege.be

Abstract: Coastal cities in the Mediterranean region have cool sea breezes that can reduce the effects of global warming, urban heat islands (UHI), and air pollution. However, in many coastal cities, impermeable urban seafront buildings prevent cool sea breezes from penetrating the city while at the same time posing a risk of pedestrian wind discomfort. This study aims to design wind-adaptive urban seafront buildings that improve urban ventilation and pedestrian wind comfort in Izmir, a high-density Mediterranean city, using the parametric design and computational fluid dynamics (CFD) method. Alternative seafront buildings consisting of two-rows and shifted configurations were designed using the two proposed urban geometric indicators. The authors found that the denser and more compact seafront building configuration can prevent the risk of wind discomfort and achieves the highest ventilation efficiency (82%). The findings apply to similar coastal urban environments and help urban policymakers and designers.

Keywords: urban seafront buildings; urban ventilation; pedestrian wind comfort; shifted building configuration; computational fluid dynamics; CFD.

Reference to this paper should be made as follows: Bas, H., Dogrusoy, I.T. and Reiter, S. (2022) 'Wind adaptive urban seafront buildings design for improving urban ventilation and pedestrian wind comfort in Mediterranean climate', *Int. J. Global Warming*, Vol. 28, No. 3, pp.239–259.

Biographical notes: Hakan Bas received his BSc from the Department of Architecture, Yildiz Technical University and MSc of Sustainable Buildings, Performance, and Design Program from Oxford Brookes University. He is currently pursuing his PhD at the Dokuz Eylul University. During his PhD, he conducted research in the Local Environment Management and Analysis (LEMA) Research Unit at University of Liege. His main research areas are building and urban aerodynamics, pedestrian wind comfort, urban ventilation and sustainable architecture.

Ilknur Turkseven Dogrusoy is a Professor at the Department of Architecture, Dokuz Eylul University. Her main research areas are architecture-urban/public space relations, sustainable architecture and human-environment studies.

Sigrid Reiter is a Professor in Architecture, Architectural Engineering, and Urban Design at the University of Liège, Belgium, from 2008. She received her Engineering degree in Architecture in 1998 and PhD in Applied Sciences in 2007 at the UCLouvain, Belgium. She is currently the Co-Director of the Local Environment Management and Analysis (LEMA) Research Team and Laboratory, which includes 24 researchers, within the Urban and Environmental Engineering (UEE) Research Unit of the University of Liège. Her research studies focus on sustainable urban design and architecture, particularly sustainable architectural and urban modelling. In April 2022, she is an author or co-author of more than 150 scientific publications.

1 Introduction

Urban areas suffer from urban heat island (UHI) effects and air pollution due to global warming and heavy urbanisation. However, wind flow can mitigate the impact of global warming and heavy urbanisation as it regulates urban temperature and reduces the intensity of the UHI effect (He et al., 2020). In particular, cool winds from the sea can play a pivotal role in reducing the stagnated heat in urban areas. In addition, wind flow also can promote urban air quality. For example, during the development of the COVID-19 pandemic, a higher number of COVID-19 cases were reported in cities with a low average wind flow velocity (Coccia, 2020).

In addition to its positive effects, wind flow can cause adverse effects on urban environments. Many coastal cities, in particular, are exposed to strong winds and, therefore, suffer from pedestrian wind discomfort risk (Johansson and Yahia, 2020). Furthermore, along with the strength of the wind, the size and shape of the buildings cause the risk of pedestrian wind discomfort.

Numerous studies investigated the effect of urban geometry on pedestrian wind comfort and urban ventilation. Reiter (2010) examined the impact of building dimensions on wind speed conditions using a parametric approach and found that wind discomfort risk was susceptible to building dimensions (height, width). In general, higher building density causes lower wind speed; however, larger passage width (Hu and Yoshie, 2013) provides more air circulation. On the other hand, the grid-aligned building configuration has higher ventilation efficiency than the shifted building configuration (Brown and DeKay, 2001).

Earlier studies confirm that large passages, low building density, and grid-aligned building configurations increase air circulation. However, narrow passages reduce air

circulation and increase the risk of pedestrian wind discomfort. In general, urban density and compactness generally contradict urban ventilation. Therefore, a compromise is needed between urban ventilation and pedestrian wind comfort requirements in the context of today's sustainable city approach, which requires a high level of urban density/compactness.

Many cities suffer from inadequate ventilation and pedestrian wind discomfort risk. However, urban policymakers only require pedestrian wind comfort assessments around new buildings. Therefore there is a need for a multi-objective urban planning strategy that requires ventilation and pedestrian wind comfort criteria. That is especially necessary for Mediterranean coastal cities. The city of Izmir (Turkey), in the Mediterranean climate, is one of them.

This study focuses on wind adaptation of seafront buildings in Mediterranean coastal cities where ventilation and pedestrian wind comfort requirements are most needed. The city of Izmir, Turkey, and, more specifically, Alsancak neighbourhood were chosen as the study area. There are many reasons for this. Izmir is under the influence of the cool sea breezes (Imbat) blowing from the Izmir Gulf [Figure 1(a)]. However, the city suffers from the UHI effect, air pollution, and pedestrian wind discomfort risk due to the inability of the built environment, especially the seafront buildings, to adapt to sea breezes. Especially the Alsancak neighbourhood [Figure 1(b)] is not suitable for bioclimatic comfort and has high air pollution values. In addition, passages directly exposed to sea breezes on the Alsancak coastline are at risk of pedestrian wind discomfort due to the large masses of seafront buildings.

Figure 1 (a) Plan view of Izmir (b) Plan view of Alsancak neighbourhood (see online version for colours)

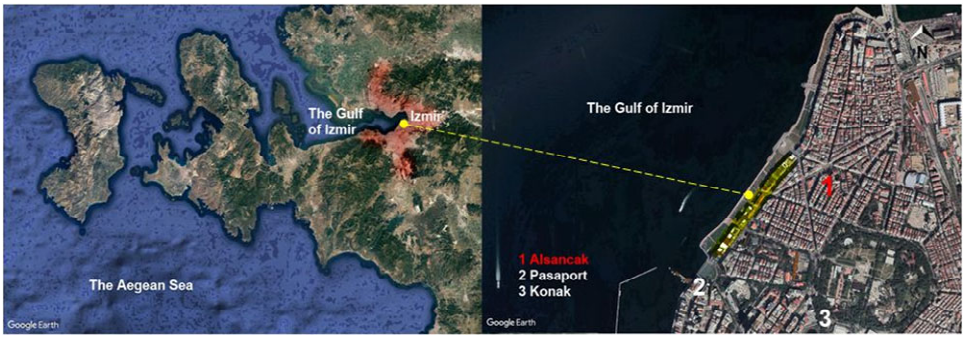

(a) (b)

Note: The yellow line represents the existing, linear seafront buildings.

Source: Adapted from Google Earth

The existing seafront buildings on the Alsancak coastline are located in the first row, where the wind interacts with the urban fabric [Figure 1(b)]. However, due to their less porous structure, they form an *urban wall* effect and reduce the natural ventilation potential of the city by preventing sea breezes. Thus, heat and polluted air accumulate in the low-rise urban areas behind the seafront buildings, resulting in poor air quality and thermal discomfort.

Site-specific urban environmental problems in Alsancak neighbourhood show that seafront buildings should be in a form that will allow the wind to enter the city while preventing the acceleration of the wind flow at the wind entrance passages. This argument shapes the objective of this study. In this context, this study aims to create an alternative design of wind-adaptive urban seafront buildings to improve urban ventilation and reduce the risk of pedestrian wind discomfort on the Alsancak coastline. However, the objective is not to derive site-specific wind solutions acting only in the city of Izmir. On the contrary, it aims to develop solutions in a generalisable and transferable format to other cities. Therefore, the overarching research question is: How can seafront buildings be designed to provide urban ventilation and pedestrian wind comfort in mid-rise, high-density, and compact Mediterranean cities?

Urban spatial planning studies can be performed at different scales. This study focuses on the seafront buildings at the urban block scale. The main reason is that the seafront buildings on the Alsancak coastline need more rehabilitation as they are denser and less porous than the inner urban areas. Also, unlike internal urban areas that usually only need ventilation due to the high density, this area needs both ventilation and pedestrian wind comfort requirements. However, considering the importance of ventilating inner urban areas with the sea breeze, the block configuration study that allows the wind effects to penetrate deep into the city will be helpful for future studies.

The present study focuses only on the sea breeze and is performed based on the site-specific conditions: the direction of the sea breeze is normal to the frontal façade of the buildings on the Alsancak coastline. Although this assumption is present in many coastlines of Izmir and other seafront cities, the results of this study should be applied only to urban areas where the wind direction is normal to the frontal façade and that are located in the Mediterranean climate.

The main contribution of this study is to determine the best possible seafront building configuration achieving the minimum wind discomfort risk and the maximum ventilation efficiency in the Mediterranean climate using the parametric design method coupled with CFD simulations. This study is expected to benefit many stakeholders. First, it will assist urban policymakers in creating wind-adaptive urban spatial planning policies in coastal urban areas. Second, it will help architects and city planners at the early design stage of the wind-adaptive building-mass design process.

Based on the above discussions, the study is structured as follows. Section 2 presents the methodology, including a description of the proposed seafront building configurations and urban geometric indicators, and then details the computational setup for computational fluid dynamics (CFD) simulations. Section 3 evaluates the risk of wind discomfort and ventilation efficiency of the proposed design configurations. Section 4 discusses the findings considering similar studies, and Section 5 presents the main results.

2 Methodology

This study develops a methodology that integrates the CFD method with the parametric design method. CFD method provides the performance evaluation of proposed seafront building configurations. The process between parametric design and the CFD method is based on the iterative approach. It continues until the best possible urban seafront building configuration is morphologically suitable for the given site conditions and provides the best performance for urban ventilation and pedestrian wind comfort.

The parametric design method begins with an extensive literature review evaluating the wind-related urban environmental problems and current design knowledge for wind adaptation of buildings. Then, urban geometric indicators and climate-based wind speed thresholds are determined by considering site-specific climatic conditions and urban context. Finally, parametric seafront building configurations are created and tested with CFD simulations. The CFD method was specifically chosen as it allows for rapid testing of parametric design variations and visualisation of the entire flow field.

2.1 Climatic considerations

The city of Izmir is located on the west coast of Turkey at 38.42°N latitude and 27.14°E longitude. The climate of Izmir is a typical Mediterranean climate, with hot and dry summers and wet and mild winters. According to the TSMS (2018), the average temperature is 10.7 °C in winter and 27.7°C in summer.

The city is under the influence of İmbat, which is a local sea breeze. Considering the climate and environmental problems of Izmir, the sea breeze is unique and of high quality compared to other winds in many ways. Since its origin is the sea, the sea breeze carries the clean and cool air mass. It is regular as it depends on the temperature difference between the sea and the land. It is faster in summer and weaker in winter. These features are desirable to reduce excessive city temperature in summer and ventilate the city with fresh air. According to the Pasaport meteorological station (TSMS), which is the closest station to the Alsancak neighbourhood [Figure 1(b)], the average annual wind speed (z = 10 m) is 3.4 m/s in winter and 4.2 m/s in summer. The direction of the sea breeze is North-Northwest, and its average annual speed is 3.64 m/s (z = 10 m).

2.2 Design of urban seafront buildings

2.2.1 Determination of climate-based target design wind speed thresholds

This study has multi-objective and needs a multi-criteria evaluation. For this reason, the upper and lower target wind speed thresholds for each objective should be determined and then optimised. Alsancak neighbourhood is the city's recreation area and contains many restaurants and cafes. Isyumon and Davenport (1975) recommend that the wind speed threshold for long-term seating on restaurant terraces should be below 3.6 m/s. On the other hand, when the wind speed is above the light breeze conditions (V > 3.3 m/s), the hair is disturbed, clothes are flapped, and the newspaper becomes hard to read according to the Beaufort scale. Accordingly, in terms of pedestrian wind comfort, the upper wind speed threshold for the long-term seating area was determined as 3.3 m/s, and gentle breeze conditions (3.4–5.4 m/s) are accepted in the walking area.

High wind speed can reduce the urban temperature (He et al., 2020). Ng (2009) stated that a light breeze of 1.0 to 1.5 m/s can provide thermal comfort for the person standing under shade when the temperature is 28°C in Hong Kong. The average temperature in Izmir in summer is 27.7°C, and therefore, at least a wind speed of 1.0 m/s is necessary to avoid thermal discomfort in summer.

High wind speed can improve urban ventilation, and a wind speed of at least 1.0 m/s is recommended as a standard for urban air pollution diffusion (Xu and Xu, 2020). Accordingly, 1.0 m/s was determined as the lower wind speed at pedestrian level (z = 2 m) for urban ventilation.

After separately evaluating the required wind speed thresholds for pollutant dilution, pedestrian thermal comfort, and pedestrian wind comfort, we optimised the target lower and upper design wind speed thresholds between 1.0 m/s and 3.3 m/s. The minimum wind speed threshold is 1.0 m/s in terms of pollutant dilution and pedestrian thermal comfort, and the maximum wind speed threshold is 3.3 m/s in terms of pedestrian wind comfort. Thus, we achieved a compromise between conflicting design wind speed requirements. In this context, the design aims to avoid two wind conditions:

1 stagnant wind flow conditions: $V < 1.0$ m/s

2 windy conditions: $V > 3.3$ m/s.

According to the *power law*, the average annual wind speed of the sea breeze is 3.64 m/s ($z = 10$ m), and this corresponds to 2.96 m/s at pedestrian level ($z = 2$ m). Therefore if the wind flow acceleration caused by the buildings is limited to a maximum of 12%, it is possible to provide the target upper wind speed threshold.

2.2.2 Description of urban seafront building configurations

The strategy in the design is to maximise urban ventilation efficiency and minimise the risk of wind discomfort. In this context, two requirements were taken into account when determining the size of the buildings:

1 Wind discomfort risk and urban ventilation efficiency: Large building width can increase the risk of wind discomfort (Reiter, 2010) and cause stagnant wind flow areas behind it. Therefore, large building widths should be avoided.

2 Cross-ventilation of buildings: A shallow building form with the building length kept as short as possible is desirable for better indoor ventilation in the Mediterranean climate.

We optimised these two requirements and proposed two rows of seafront buildings. The width and length of the buildings are 20 m and 10 m in the first row (Figure 2), and the height of the buildings is 25 m, representing mid-rise buildings in Izmir and many dense European cities. In addition, the street width between the first-row buildings is 10 m to allow walking and long-term seating activities.

The second-row buildings were designed with a parametric approach. First, we created five urban geometric indicators consisting of four separate (W, S_{x1}, S_{x2}, S_y) and one interrelated (W/S_{x1}) where W is the width of the downwind buildings, S_{x1} is the passage width between upwind buildings, S_{x2} is the passage width between downwind buildings, and S_y is the actual passage width between upwind and downwind buildings (Figure 2).

We determined five different building widths (W) consisting of 8, 12, 16, 20, and 24 m for the second-row buildings. These building widths correspond to aspect ratios (W/S_{x1}) of 0.8, 1.2, 1.6, 2.0, and 2.4, respectively, where S_{x1} is constant and 10 m. Five aspect ratios were matched with five block spacing widths (S_y) of 4, 5, 6, 8, and 10 m. Thus, 25 different hypothetical seafront building configurations were created. Figure 3 shows the 3D view of the designed seafront building configurations. Depending on the variables, there is a parametric relationship between the configurations. From left to right, W/S_{x1} increases, and from top to bottom (S_y) decreases.

Figure 2 Description of the urban geometric indicators in plan view (see online version for colours)

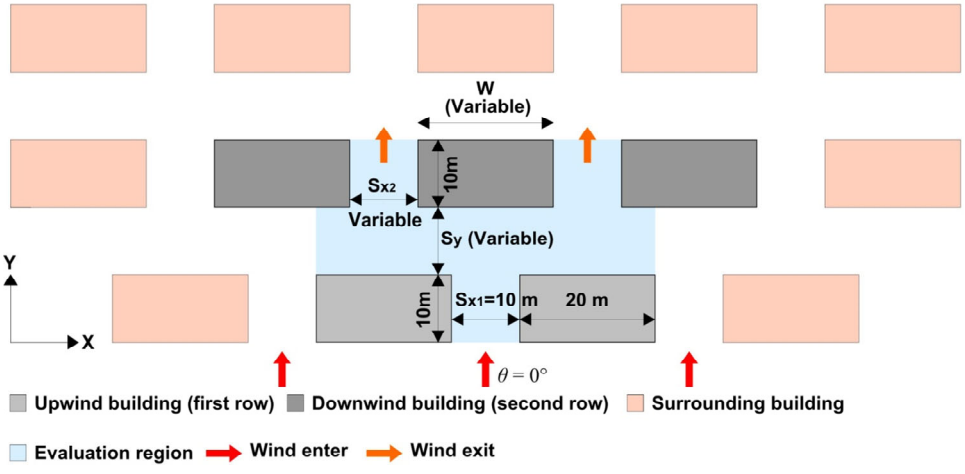

Figure 3 3D view of twenty-five urban seafront building configurations (see online version for colours)

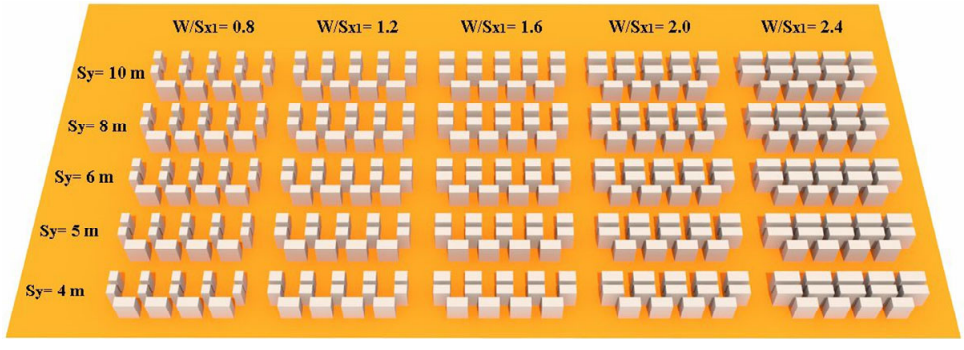

This study focuses on dense and compact coastal urban areas; therefore, we determined the density/compactness levels of urban seafront building configurations using the standardised, climate-based classification of Stewart and Oke (2012). In this classification system, the aspect ratio (mean height-to-width ratio of street canyons – H/W) and the building surface fraction (BSF) (ratio of building plan area to total plan area – %) are two fundamental indicators. For the compact-midrise category, the aspect ratio (H/W) should be higher than 1, and the BSF should be between 40% and 70% (Stewart and Oke, 2012). As street widths are variable in seafront building configurations, aspect ratio and BSF change parametrically. In the first row, the aspect ratio (H/S_{x1}) is constant and equals 2.5, which refers to a highly dense and compact type of urban geometry. In the second row, the aspect ratio is variable for the x (H/S_{x2}) and y (H/S_y) directions. The BSF of the building configurations varies between 31% and 61%. From left to right and from top to bottom, the density/compactness level of the seafront building configurations increases.

2.2.3 Evaluation of urban ventilation efficiency and pedestrian wind comfort

This study mainly aims at architects and city planners, so it is necessary to use a practical quantitative evaluation parameter. Therefore, we used the widely accepted indicator of wind velocity ratio (VR_w) to evaluate pedestrian-level urban ventilation efficiency. VR_w is the ratio of wind velocity at the pedestrian level to the free stream velocity of the boundary layer (Gülten and Öztop, 2020).

$$VR_w = V/V_{ref} \tag{1}$$

where V = mean wind velocity at the measuring point (z = 2 m) and V_{ref} = free stream mean wind velocity. The higher the VR_w value, the higher the urban ventilation efficiency. We considered the free stream velocity (V_{ref}) at 2 m height from the ground, and we used the following equation [equation (2)] to evaluate the predictive ventilation efficiency quantitatively:

$$Ventilation\ efficieny\ (\%) = \frac{Area\ of\ \ flow\ region\ \left(V/V_{ref}\ \geq 0.34\right)}{Area\ of\ \ total\ evaluation\ region} \times 100\% \tag{2}$$

The wind velocity ratio (VR_w) was also used to evaluate pedestrian wind comfort. However, higher VR_w values indicate a higher risk of pedestrian wind discomfort.

2.2.4 Distribution of measuring points

Pedestrian street use was taken into account when determining the location of the measuring points. The street centre axis is used for pedestrian walking, and the 2.5 m wide areas on both sides of the streets are used for long-term seating activities by restaurants and cafes in Alsancak neighbourhood.

Potential locations of the high-speed regions were also considered in determining the location of measuring points. Critical locations are the building corners and the passage centre axis (PCA). The measuring points were located along the passage centre axis representing the pedestrian walking area and the potential location of the *double corner effect*. They were also located 1.25 metres from the buildings along the central axis of the long-term seating area (SCA), representing the potential location of the *corner effect*. The measuring points are in the same configuration in all three different passages.

2.3 CFD setup

The CFD setup was created using the best practice guidelines (BPGs) (Franke et al., 2004, 2007), and the CFD results were validated with experimental data.

2.3.1 CFD validation

We used wind tunnel dataset files (Excel) provided by the working group of the AIJ (2016) for CFD validation. The datasets file contains test results, inflow boundary conditions, and measurement points. Datasets were generated in the 3 m wide, 1.8 m high, and 22 m long wind tunnel at the Fujita Technology Center.

We used the sub-case (case 1 H) of configuration C proposed by AIJ (2016) for validation. Case 1 H consists of nine uniform urban blocks in a grid-aligned

configuration. The dimensions of the buildings (width: depth: height) and the passage widths are 20 m. Wind velocity was measured at 2 m height from the ground.

2.3.1.1 Boundary conditions

The lateral and top size of the computational boundary is limited to wind tunnel sizes: 1.8 m (9 H) height and 3.0 m (15 H) width, where H is the building height. The wind tunnel dimensions limit the distance between the tunnel boundary and the central area of interest to 8 H (top) and 5 H (lateral). The inlet boundary is located at 10 H, and the outflow boundary is located 15 H from the central area of interest (Franke et al., 2007).

The inlet wind velocity U (m/s) and the RMS value of velocity fluctuation σ_u (m/s) for lower parts of the ABL (0–120 m) were provided from the experimental data, and the turbulence kinetic energy $k(z)$ was calculated using the RMS value of velocity fluctuation:

$$k(z) \cong \sigma_u^2(z) \tag{3}$$

The turbulence dissipation (ε) was calculated from the relation $P_k = (\varepsilon)$ (P_k: production term for k equation):

$$\varepsilon(z) = Pk(z) = C_\mu^{1/2} \cdot k(z) \cdot dU(z)/dz, \text{ where } C_\mu \text{ is the model constant } (= 0.09) \tag{4}$$

In modelling the ground surface boundary conditions, the equivalent sand-grain roughness height (k_s) was calculated using equation (5) (Blocken et al., 2007):

$$k_s = \frac{9.793 * z_0}{c_s} \tag{5}$$

where the value 9.793 is the empirical wall constant E (–), and the value of 1.0 is the c_s (roughness constant).

The value of roughness length (z_0) to be used in equation (5) was calculated using equation (6):

$$\frac{U_{ref}}{u^*} = \frac{1}{k} \ln\left(\frac{z_{ref}}{z_o}\right) \tag{6}$$

where the von Karman constant (κ) was taken as 0.41.

u^* friction velocity at the height of z_{ref} (= 0.01 m) was calculated using the formula:

$$u^* \cong C_\mu^{\frac{1}{4}} \sqrt{k} = 0.09^{\frac{1}{4}} \sqrt{0.314} = 0.307 \text{ m/s} \tag{7}$$

The value of z_0 was found to be 4.386×10^{-4}. Using the z_0 value in equation (5), k_s was found 4.3×10^{-3} m on the experimental scale.

No-slip and smooth wall boundary conditions for building surfaces; and slip/symmetrical wall boundary conditions for the lateral and upper boundaries were imposed. In addition, zero static pressure was specified at the outlet boundary.

2.3.1.2 Turbulence model

We used steady-state Reynolds-averaged Navier Stokes (RANS) equations to estimate mean wind speed and an explicit turbulence model to calculate the effect of turbulence on mean wind speed. We compared the standard $k - \varepsilon$, realisable $k - \varepsilon$, and Reynolds stress model (RSM) under the same calculation conditions to find the most suitable turbulence model. The flow was assumed to be turbulent and incompressible.

2.3.1.3 Grid generation

A grid independence test was conducted by considering three requirements. First, at least ten grids should be used on one side of the building. Second, at least 2 or 3 grids should be present at pedestrian level (0–2 m) (Franke et al., 2004). Third, the distance y_P [the centre point (P) of the first grid] should be greater than k_s (Blocken et al., 2007). In this context, the building with a side of 20 m should have a grid size of at most 2 m, and the height of the first grid should be equal to or less than 1 m for pedestrian level assessment at 2 m. Also, since k_s is equal to 0.43 m, the height of the first grid should be greater than 0.86 m. However, it is difficult to provide three different grids that satisfy these conditions. Therefore, we compared the grid sizes of 2 m (10 grids), 1.25 (16 grids) m, and 1 m (20 grids). Among them, 1 m grid size satisfies the three requirements and includes at least two grids at pedestrian level (0–2 m).

In the grid independence test, we used structured hexahedral cells and applied a local grid refinement in the area of interest. For the 1 m grid test, the grid size is 1 m at the central area of interest and gradually increases with distance from the central area of interest, reaching a maximum of 8 m.

We used the linear pressure strain (RSM) turbulence model of STAR as the other calculation settings. We applied a high y^+ ($30 < y^+ < 150$) wall treatment method, and we also used fifteen boundary layer elements with a stretching ratio of 1.2 to resolve the near-wall boundary layer. We used the segregated flow model of STAR based on the SIMPLE algorithm.

The grid independence test shows that the 2 m grid does not fit the experiment results, and the grid should be at least 1.25 m or less for better agreement with the experimental results. However, we used the 1 m grid to meet all the requirements recommended by BPGs.

Figure 4 Comparison of wind velocity ratios between experiment and CFD according to different turbulence models (see online version for colours)

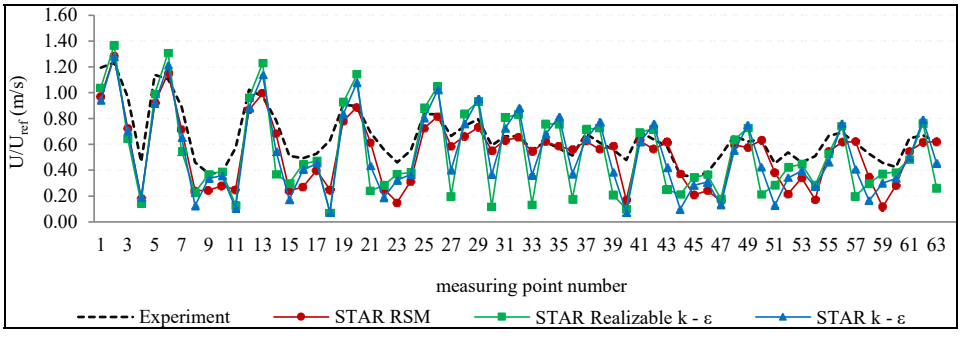

We simulated configuration C (AIJ, 2016) for CFD validation, and we compared the wind speed ratios (U/U_{ref}) with the experiment results (Figure 4). All turbulence models underestimated the wind speed ratios in the low-speed region. But overall, RSM is more accurate than other turbulence models. In the region where $U/U_{ref} > 0.6$, the percent error is around 10.8% for RSM, while 21.4% and 26.5% for standard $k - \varepsilon$ and realisable $k - \varepsilon$, respectively. All turbulence models accurately simulated the highest velocity region. In the highest wind speed region where $U/U_{ref} > 1.0$, we found the percent error of RSM, standard $k - \varepsilon$, and realisable $k - \varepsilon$ are 12%, 12.2%, and 13.2%, respectively.

2.3.2 CFD setup for simulating urban seafront building configurations

2.3.2.1 Domain size

The domain size was calculated to avoid the blockage effect. We first determined the top size as 8 H. Thus, keeping the blockage ratio below 3%, we set the lateral dimension as 12 H. In addition, we set the inlet and outflow boundaries from the central area of interest as 10 H and 15 H, respectively (Franke et al., 2004).

2.3.2.2 Boundary conditions

The study area in Alsancak neighbourhood is near the sea, and there is a large and low-grass covered area between the seafront buildings and the sea. The aerodynamic roughness length (z_0) of low-grass is 0.01, and the power-law exponent (α) for such a terrain category is 0.13 (Burton et al., 2012).

Using the mean wind speed (U_{ref}) obtained from Pasaport/Izmir meteorological station (TSMS) and power-law exponent (α) in a simple *power-law* equation, the vertical wind velocity profile was generated for the study area.

We used the formula proposed by Richards and Hoxey (1993) to generate the turbulence parameters in the type of k (turbulence kinetic energy) + ε (turbulence kinetic energy dissipation):

$$U(z) = \frac{u^*}{\kappa} \ln + \left(\frac{z + z_g}{z_0} \right) \tag{8}$$

$$k(z) = \frac{u^{*2}}{\sqrt{c_\mu}} \tag{9}$$

$$\varepsilon(z) = \frac{u^{*3}}{\kappa (z + z_O)} \tag{10}$$

where U_z is the mean wind speed, u^* is the ABL friction velocity, z is the height from the ground, z_0 is the aerodynamic roughness length, κ is the von Karman constant, k is the turbulence kinetic energy, C_μ (= 0.09) is a model constant, and ε is the turbulence dissipation rate.

The ground surface boundary condition was calculated using equation (5), and the equivalent sand-grain roughness height (k_s) was found as 9.8×10^{-2} m. We applied no-slip and smooth wall boundary conditions on building surfaces and slip/symmetrical wall boundary conditions on the lateral and upper boundaries. Zero static pressure was used at the outlet boundary.

2.3.2.3 Other parameters

We retained the 1 m grid size and constructed the grid with structured hexahedral cells. We used STAR's RSM turbulence model in the simulations.

3 Results

The CFD simulations were performed, and the wind velocity ratio (VR_w) was measured in three passages (passages 1, 2, and 3).

3.1 Wind discomfort assessment in passage 1

Passage 1 is located between upwind buildings, and maximum wind velocity ratios (VR_w) range from 0.98 to 1.36 at PCA_1 [Figure 5(a)]. Six building configurations (conf. 19, 20, 21, 22, 23, 24, and 25) provide the upper wind speed thresholds ($VR_w \leq 1.12$). However, the best wind climate is achieved by conf. 25 ($W/S_{x1} = 2.4$, $S_y = 4$ m). This configuration completely prevents the wind discomfort risk (double corner effect) at PCA_1 and slows down the wind flow by 2% ($VR_w = 0.98$). On the contrary, the worst wind climate with a 1.36 VR_w is provided by conf. 1 ($W/S_{x1} = 0.8$, $S_y = 10$ m).

Figure 5 Maximum wind velocity ratios (VR_w) in the horizontal plane ($z = 2$ m), (a) PCA_1 (b) SCA_1 (see online version for colours)

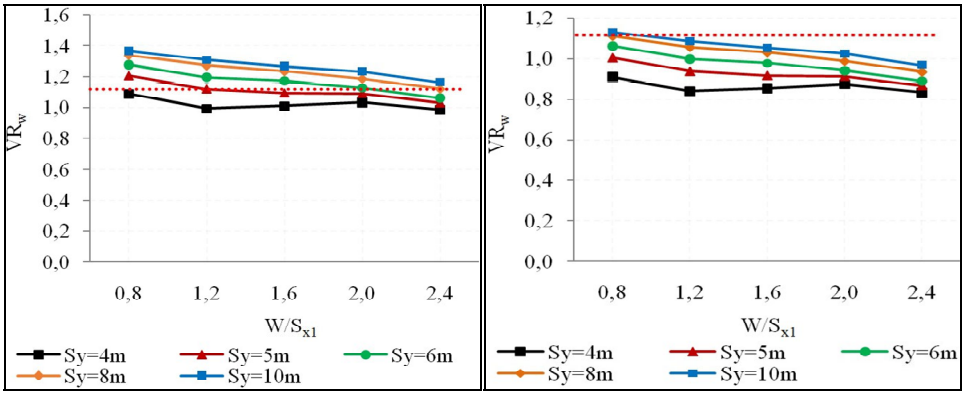

(a) (b)

Note: Red dashed line corresponds to upper target wind speed threshold (VR_w =1.12).

We found two strong correlations: the first is between W/S_{x1} and VR_w and the second is between S_y and VR_w. Parametrically, as the aspect ratio of W/S_{x1} increases, VR_w decreases at PCA_1. On the contrary, as S_y increases, VR_w increases at PCA_1. It should be emphasised that S_y is a more effective geometric indicator for reducing flow acceleration at PCA_1 than W/S_{x1}. When S_y is 4 m, all configurations meet the upper wind design threshold ($VR_w \leq 1.12$) regardless of the W/S_{x1}.

Wind discomfort risk was also evaluated at SCA_1. The maximum wind velocity ratio (VR_w) is lower at SCA_1 than at PCA_1 [Figure 5(b)]. The VR_w at SCA_1 is below 1.12 in all configurations, and therefore, all configurations are wind comfortable for the long-term

seating activity. A higher W/S_{x1} ratio and lower S_y provide lower VR_w at SCA_1. The best wind climate (VR_w = 0.82) is achieved by conf. 25.

3.2 Wind discomfort assessment in passage 2

Passage 2 is the wind exit passage between parallel downwind buildings. Maximum wind velocity ratios (VR_w) range from 0.75 to 1.03 at PCA_2 and do not exceed the upper wind speed threshold ($VR_w \leq 1.12$). Therefore, there is no wind discomfort risk at PCA_2 for all configurations [Figure 6(a)].

Figure 6 Maximum wind velocity ratios (VR_w) in the horizontal plane (z = 2 m), (a) PCA_2 (b) SCA_2 (see online version for colours)

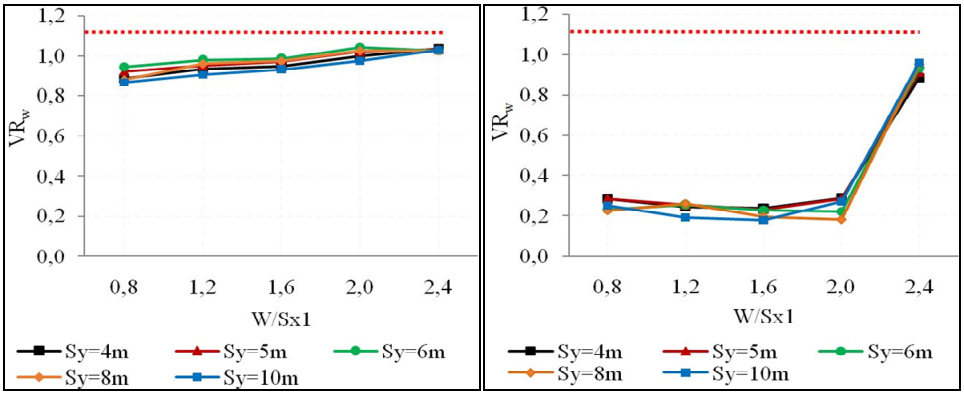

(a) (b)

Although there is no direct correlation between S_y and VR_w, it does exist between W/S_{x1} and VR_w: as W/S_{x1} increases, so does VR_w. It should be noted that when W/S_{x1} increases, S_{x2} decreases, and passage 2 becomes narrower. The *Venturi effect* can explain this finding, which means that the wind speed in narrow passages will be higher than in wide passages.

The maximum VR_w at SCA_2 is below the upper wind speed threshold ($VR_w \leq 1.12$) in all configurations [Figure 6(b)]. However, VR_w increases significantly when W/S_{x1} is 2.4. Conf. 5, 10, 15, 20, and 25 have the highest VR_w value of 0.89 to 0.96. In these configurations, passage width (S_{x2}) decreases to 6 m, and the flow interaction developed at PCA_2 interacts with the more stagnant flow region of SCA_2. Thus, VR_w at SCA_2 significantly increases.

3.3 Wind discomfort assessment in passage 3

Passage 3 is the parallel passage to the wind flow direction and connects passages 1 and 2. Maximum wind velocity ratios (VR_w) at PCA_3 range from 0.61 to 0.99 [Figure 7(a)], and all configurations provide the upper design wind speed threshold ($VR_w \leq 1.12$). There is not a direct correlation between S_y and VR_w. However, in very narrow passages where S_y is 4–5 m, VR_w is relatively higher.

In general, PCA_3 is wind comfortable, but local flow acceleration occurs at the corner of downwind buildings (SCA_3). At these locations, VR_w can reach 1.26 when S_y is 4 m

[Figure 7(b)]. Local wind flow acceleration will be explained in detail in the following subsection.

Figure 7 Maximum wind velocity ratios (VR_w) in the horizontal plane (z = 2 m), (a) PCA_3 (b) SCA_3 (see online version for colours)

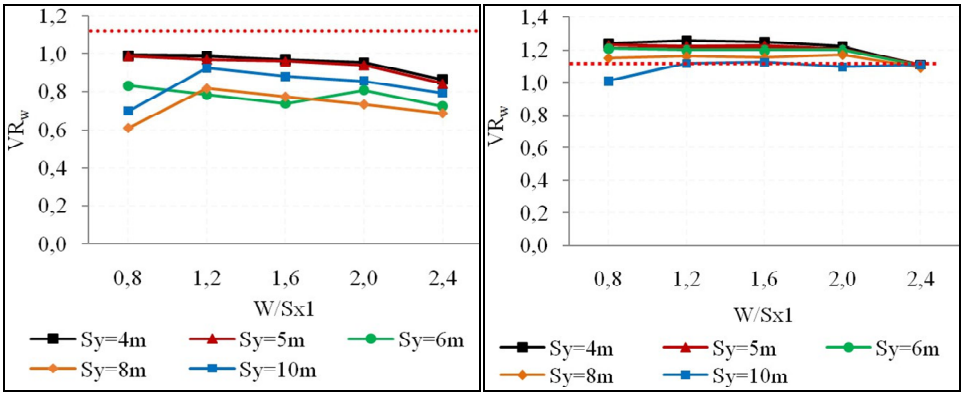

(a) (b)

3.4 *Ventilation efficiency assessment of seafront building configurations*

In ventilation efficiency assessment, we found strong positive correlations between W/S_{x1}, S_y, and VR_w. In general, the increase of W/S_{x1} and S_y increases ventilation efficiency (Figure 8). The ventilation efficiency of the building configurations ranges from 54% to 82% in the evaluation region, and the highest ventilation efficiency is achieved by conf. 25. In this configuration, the lower wind speed threshold ($VR_w \geq 0.34$) is exceeded in 82% of the evaluation region.

Figure 8 Ventilation efficiency (%) in the evaluation region, in the horizontal plane (z = 2 m) (see online version for colours)

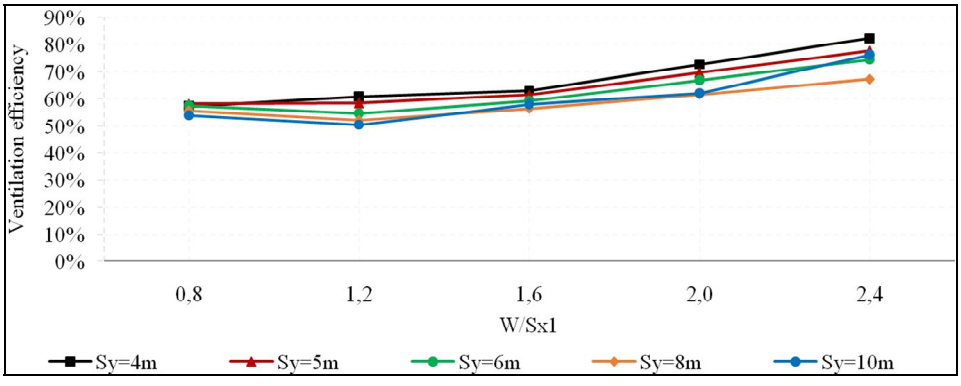

3.5 Wind discomfort and ventilation efficiency assessment of the best possible seafront building configurations

Pedestrian wind discomfort and ventilation efficiency assessments show many configurations satisfy the target design wind speed thresholds. However, according to the multi-objectives of this study, the best possible seafront building configuration is the one that performs better in the entire evaluation region (passages 1, 2 and 3) in terms of wind discomfort risk and ventilation efficiency. It is noteworthy that there is no conflict between pedestrian wind discomfort risk and ventilation efficiency in determining the best possible seafront building configuration. Unlike other configurations, conf. 20 and 25 achieve a better wind environment in the evaluation region. For these configurations, W/S_{x1} is 2.4, and S_y is 4 and 5 m for the conf. 20 and conf. 25, respectively. Although both satisfy the target design wind speed thresholds in the evaluation region, conf. 25 has a lower risk of wind discomfort and provides higher ventilation efficiency than conf. 20.

Figure 9 Wind velocity distribution around, (a) conf. 25 (b) wind discomfort risk (c) ventilation efficiency (see online version for colours)

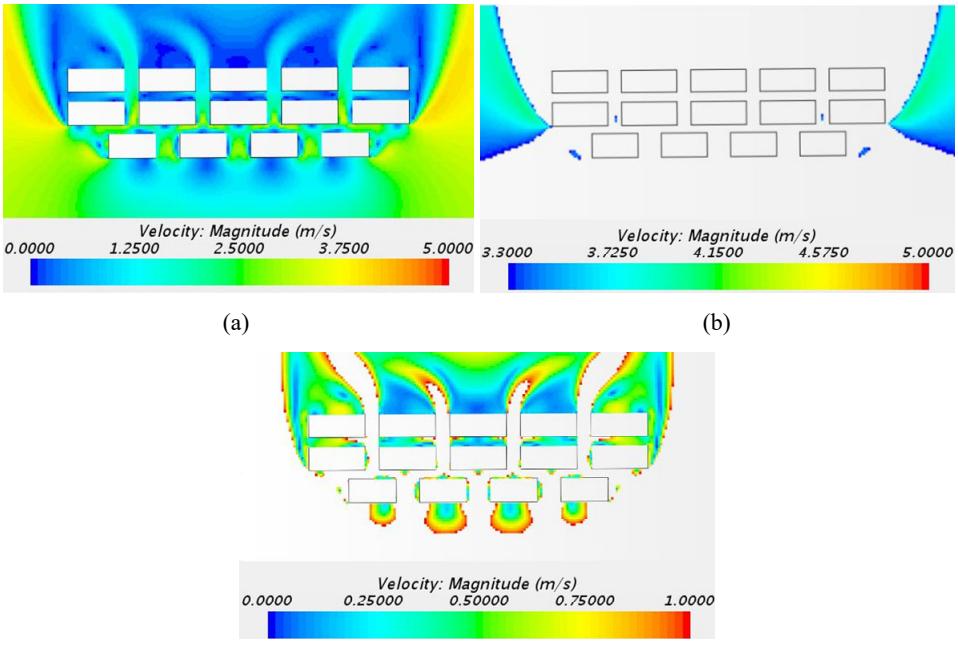

A detailed analysis was performed for conf. 25 visualising the entire evaluation region. Figure 9(a) shows the contour plots of velocity magnitude at pedestrian level (z = 2 m), and Figure 9(b) shows the risk of wind discomfort. The blank spaces in Figure 9(b) show VR_w below 1.12, corresponding to wind velocities below 3.3 m/s. VR_w never exceeds the upper design wind speed threshold ($VR_w \leq 1.12$). Figure 9(c) shows the contour plots of velocity magnitude where the wind speed is below 1.0 m/s ($VR_w \leq 0.34$). According to Figure 9(c), conf. 25 does not completely prevent the stagnant wind flow area in the evaluation region. An area of approximately 1 m wide around the upwind buildings has a

stagnant wind environment [Figure 9(c)] due to the *boundary layer effect* of the buildings.

Conf. 25 has the highest density/compactness, with the highest aspect ratios (H/S_{x2} = 4.2; H/S_y = 6.3) and BSF (61%). It is noteworthy that the more compact and denser seafront building configuration is the best possible one for pedestrian wind comfort and urban ventilation. However, passage 2 is 6 m wide in this configuration, and passage 3 is 4 m wide. These passage widths are not functional for both long-term seating and pedestrian walking activities at the same place. Therefore, although this configuration performs best for all objectives, it is not functional from urban planning aspects.

On the other hand, while the configuration with all passage widths of 10 m (conf. 4) is more functional, it cannot meet the target wind speed thresholds and does not prevent the risk of wind discomfort in passage 1. Therefore, a compromise must be provided between the passage function, pedestrian wind comfort, urban ventilation efficiency, and density/compactness. In conf. 19, passage 2 is 10 m wide, and passage 3 is 5 m, providing an acceptable wind environment from wind discomfort risk and ventilation efficiency aspects. Therefore, a detailed analysis was performed for conf. 19, which visualised the entire evaluation region.

Figure 10 Wind velocity distribution around, (a) ref. conf. 19 (b) wind discomfort risk (c) ventilation efficiency (see online version for colours)

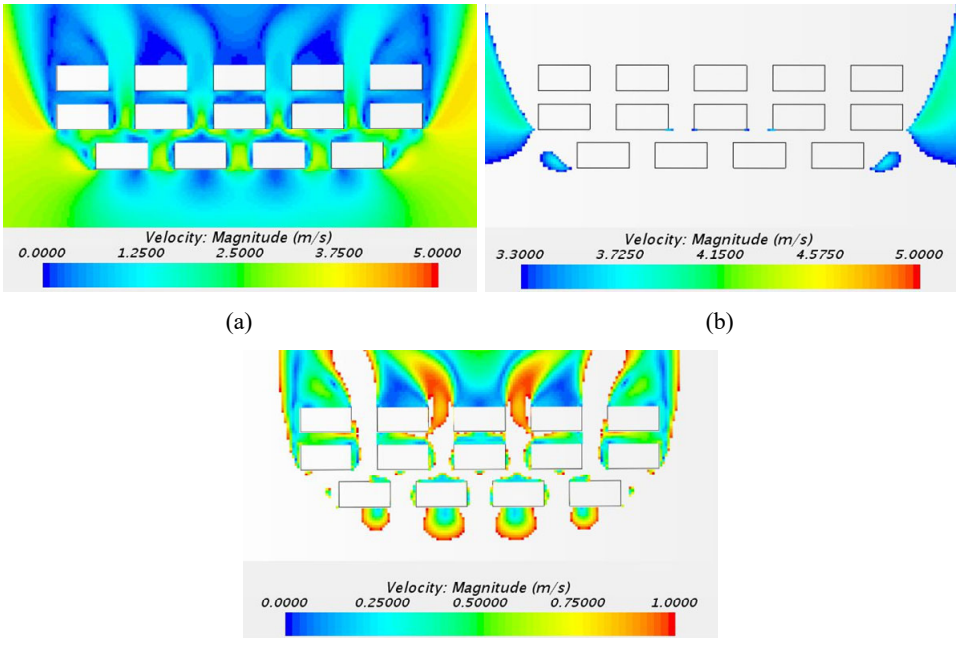

Figure 10(a) shows the contour plots of velocity magnitude at pedestrian level (z = 2 m) for conf. 19, and Figure 10(b) illustrates the risk of wind discomfort. In general, conf. 19 meets the upper design wind speed threshold; however, it cannot prevent local flow acceleration (21%) at the corners of downwind buildings (SCA_3). However, since the local flow acceleration takes place in a limited area, the risk of pedestrian wind

discomfort was minimised. The ventilation efficiency was assessed in Figure 10(c), which shows the contour plots of velocity magnitude where the wind speed is below 1.0 m/s ($VR_w \leq 0.34$). The ventilation efficiency of conf. 19 (64%) is 18% less than the ventilation efficiency of conf. 25 (82%).

This study proposed alternative options for existing seafront buildings on the Alsancak coastline. Figure 11 shows the typical seafront buildings in the Alsancak coastline consisting of an enclosed, single block that fully utilises the site and the alternative designed options (conf. 25 and conf. 19) together. The alternative designed configurations have a more porous form to wind flow to mitigate UHI and air pollution and have wind comfortable passages. They also do not neglect to provide density/ compactness of the urban form. The Mediterranean climate requires more permeable buildings. Therefore, in terms of architecture and urban planning, such a comparison is necessary to show how an enclosed linear block located along the coast should be fragmented and how and in what configuration urban open spaces should be placed between buildings for pedestrian wind comfort and urban ventilation.

Figure 11 Plan view of existing and proposed alternative urban seafront building configurations (see online version for colours)

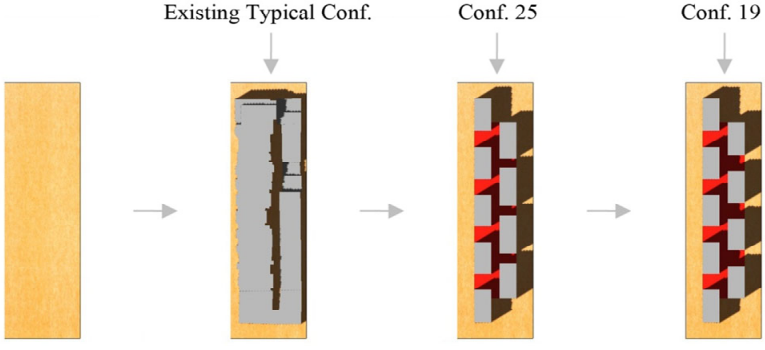

4 Discussion

Numerous studies focused on fulfilling a single criterion, such as pedestrian wind comfort or urban ventilation in urban spatial planning. However, this study aims to fulfil both criteria simultaneously; therefore, the contradictions encountered in fulfilling both requirements should be discussed.

4.1 Role of building configuration on the risk of wind discomfort risk and ventilation efficiency

This study proposes alternative design options for the existing urban seafront buildings in Alsancak neighbourhood. Given that seafront buildings are exposed to open wind conditions, the risk of wind discomfort at passages is unavoidable. On the other hand, although wide passages promote ventilation (Hu and Yoshie, 2013), they are not sufficient to prevent the risk of wind discomfort at passages. We found that establishing a mutual relationship between the first-row and second-row seafront buildings based on

two geometric indicators (higher W/S_{x1} ratio and lower S_y) in shifted configuration has a notable effect on reducing wind speed without neglecting ventilation efficiency.

Numerous studies examining the effect of building configuration on urban ventilation reported that shifted building configuration has lower ventilation efficiency than the grid-aligned configuration (Brown and DeKay, 2001). Gülten and Öztop (2020) compared the urban block typologies using the 5 × 6, 5 × 5, 5 × 2, 4 × 3 idealised building arrays, while Chen et al. (2021) compared grid-aligned and shifted building configurations using 5 × 5 idealised building arrays. It should be noted that earlier studies were performed on a larger scale. In these studies, wind flow significantly decreases due to the large frictional drag of shifted building configuration. However, this study is on the urban block scale consisting of only two rows of buildings in the city's coastal areas. The proposed two-row shifted seafront building configurations provide high ventilation efficiency. Because the wind is strong on the coast and the two rows shifted building configuration does not create much frictional drag compared to those with more rows of buildings. This shows that the location, scale, and the number of buildings arranged can considerably affect the results. However, this study needs to be extended to the macroscopic city scale in future studies.

Earlier studies on the shifted configuration did not parametrically test the effect of urban geometric indicators on ventilation efficiency. However, in this study, the parametric design method allowed us to find the best possible shifted building configuration by eliminating other building configuration options. This shows the importance of examining the building configuration and urban geometric indicators together and parametrically.

Many studies tested the effect of building configuration on the risk of wind discomfort. They reported that shifted building configuration could cause extreme windy conditions due to the *pressure short-circuiting effect* (Janssen et al., 2013). However, it should be underlined that earlier studies investigated the risk of wind discomfort between two parallel-shifted buildings. Therefore, it should be stated that the number of the buildings in shifted configuration and particularly spacing sizes between buildings (S_{x1}, S_{x2}, and S_y) can cause different results.

Each climate has its unique climate and wind conditions, so typical urban building configurations may not work efficiently in all wind conditions. However, the adaptation of the building configuration to the unique wind conditions can be achieved with the design and modification. For example, the shifted building configuration is recommended in cold northern climates (Johansson and Yahia, 2020) to block the cold winds and avoid the formation of wind channels. In a similar approach, shifted building configuration is also recommended in hot-arid climates to prevent the free flow of hot and dusty desert wind in urban open spaces (Gut and Ackerknecht, 1993). However, the Mediterranean climate is different. Wind (sea breeze) is cool and thus desirable to regulate urban temperature. On the other hand, the risk of pedestrian wind discomfort should be prevented in the coastal passages. Therefore, the free flow of wind should be allowed while blocking the acceleration of the wind flow at the coastal passages.

The integrated use of the shifted building configuration and the two proposed urban geometric indicators in the Mediterranean coastline are critical. Such a strategy block wind flow acceleration, not wind flow. In this way, a balance is achieved between different design requirements. In this context, this study shows a way to adapt the shifted building configuration to the unique climatic and wind characteristics of the Mediterranean climate, using a parametric design method in coastal urban environments.

4.2 Role of urban density and compactness on the risk of wind discomfort risk and ventilation efficiency

The compact city paradigm generally contradicts urban ventilation (Brown and DeKay, 2001). This study supports compact and dense urban development as the more compact and denser seafront building configuration (conf. 25) performs better from pedestrian wind comfort and urban ventilation aspects. However, it should be highlighted that the findings are limited to the seafront urban buildings.

5 Conclusions

This study has presented an alternative design of urban seafront buildings to mitigate UHI and air pollution with ventilation and minimise the risk of pedestrian wind discomfort in Izmir, a dense and compact Mediterranean city.

The main conclusion is that two-row seafront buildings in the shifted configuration designed using the proposed urban geometric indicators (W/S_{x1}, S_y) can prevent the *double corner effect* and maximise urban ventilation efficiency (82%).

Two findings should be highlighted. First, to achieve the minimum wind discomfort risk and maximum ventilation efficiency in coastal urban open areas, three factors should be provided together:

1 shifted building configuration

2 higher W/S_{x1}

3 lower S_y.

Second, there is a strong positive correlation between increasing the density/compactness of the seafront building configurations and improving pedestrian wind comfort and urban ventilation efficiency. The results show a compromise between pedestrian wind comfort and ventilation efficiency requirements without neglecting urban density/compactness in the seafront urban area.

The pedestrian-level wind climate can be improved in the coastal part of Izmir with the application of the findings. The results also apply to other coastal cities, and the findings can be generalised to similar coastal urban environments since the study creates new empirical building spacing rules. Urban wind flow is associated with many urban environmental issues such as global warming, UHI, air pollution, and pedestrian wind comfort, so it must be addressed holistically.

Acknowledgements

This work was financially supported by the University of Liege LEMA Research Unit, Dokuz Eylül University BAP unit (Grant No. 2020.KB.FEN.013) and the Scientific and Technological Research Council of Turkey (TUBITAK) within the scope of the 2214-A – International Research Scholarship Program for Doctoral Students.

References

Architectural Institute of Japan (AIJ) (2016) *AIJ Benchmarks for Validation of CFD Simulations Applied to Pedestrian Wind Environment around Buildings*, Architectural Institute of Japan, Tokyo.

Blocken, B., Stathopoulos, T. and Carmeliet, J. (2007) 'CFD simulation of the atmospheric boundary layer: wall function problems', *Atmospheric Environment*, Vol. 41, No. 2, pp.238–252.

Brown, G.Z. and DeKay, M. (2001) *Sun, Wind & Light: Architectural Design Strategies*, 2nd ed., Wiley, New York.

Burton, T., Sharpe, D., Jenkins, N. and Bossanyi, E. (2012) *Wind Energy Handbook*, Vol. 2, Wiley, New York.

Chen, G., Rong, L. and Zhang, G. (2021) 'Impacts of urban geometry on outdoor ventilation within idealized building arrays under unsteady diurnal cycles in summer', *Building and Environment*, Vol. 206, No. 108344, pp.1–17.

Coccia, M. (2020) 'How (un) sustainable environments are related to the diffusion of COVID-19: the relation between coronavirus disease 2019, air pollution, wind resource and energy', *Sustainability*, Vol. 12, No. 22, p.9709.

Franke, J., Hellsten, A., Schlünzen, H. and Carissimo, B. (2007) *Best Practice Guideline for the CFD Simulation of Flows in the Urban Environment. COST action 732. Quality Assurance and Improvement of Meteorological Models*, University of Hamburg, Meteorological Institute, Center of Marine and Atmospheric Sciences.

Franke, J., Hirsch, C., Jensen, A.G., Krüs, H.W., Schatzmann, M., Westbury, P.S. and Wright, N.G. (2004) 'Recommendations on the use of CFD in predicting pedestrian wind environment', in *Cost Action C*, Vol. 14, pp.1–12.

Gülten, A. and Öztop, H.F. (2020) 'Analysis of the natural ventilation performance of residential areas considering different urban configurations in Elazığ, Turkey', *Urban Climate*, Vol. 34, No. 100709, pp.1–16.

Gut, P. and Ackerknecht, D. (1993) *Climate Responsive Buildings: Appropriate Building Construction in Tropical and Subtropical Regions*, SKAT, St. Gallen.

He, B.J., Ding, L. and Prasad, D. (2020) 'Relationships among local-scale urban morphology, urban ventilation, urban heat island and outdoor thermal comfort under sea breeze influence', *Sustainable Cities and Society*, Vol. 60, No. 102289, pp.1–20.

Hu, T. and Yoshie, R. (2013) 'Indices to evaluate ventilation efficiency in newly-built urban area at pedestrian level', *Journal of Wind Engineering Industrial Aerodynamics*, Vol. 112, pp.39–51.

Isyumon, N. and Davenport, A. (1975) 'The ground level wind environment in built-up areas', in *Proceedings of the 4th International Conference on Wind Effects on Buildings and Structures*, Heathrow, UK, pp.403–422.

Janssen, W.D., Blocken, B. and van Hooff, T. (2013) 'Pedestrian wind comfort around buildings: comparison of wind comfort criteria based on whole-flow field data for a complex case study', *Building and Environment*, Vol. 59, pp.547–562.

Johansson, E. and Yahia, M.W. (2020) 'Wind comfort and solar access in a coastal development in Malmö, Sweden', *Urban Climate*, Vol. 33, No. 100645, pp.1–14.

Ng, E. (2009) 'Policies and technical guidelines for urban planning of high-density cities – air ventilation assessment (AVA) of Hong Kong', *Building and Environment*, Vol. 44, No. 7, pp.1478–1488.

Reiter, S. (2010) 'Assessing wind comfort in urban planning', *Environment and Planning B: Planning and Design*, Vol. 37, No. 5, pp.857–873.

Richards, P. and Hoxey, R. (1993) 'Appropriate boundary conditions for computational wind engineering models using the k-epsilon turbulence model', *Journal of Wind Engineering and Industrial Aerodynamics*, Vol. 46, No. 47, pp.145–153.

Stewart, I.D. and Oke, T.R. (2012) 'Local climate zones for urban temperature studies', *Bulletin of the American Meteorological Society*, Vol. 93, No. 12, pp.1879–1900.

Turkish State Meteorological Service (TSMS) (2018) *Climate Data*, Turkey [online] https://www.mgm.gov.tr/veridegerlendirme/il-ve-ilceler-istatistik.aspx?m=IZMIR (accessed 10 October 2018).

Xu, Q. and Xu, Z. (2020) 'What can urban design learn from changing winds?', *The Journal of Public Space*, Vol. 5, No. 2, pp.7–22.